
Research Paper

Cytotoxic Properties of Tyloxapol

Jung-hua Steven Kuo,^{1,4} Ming-shiou Jan,² and Hsuan Wen Chiu³

Received September 2, 2005; accepted February 28, 2006

Purpose. Tyloxapol, a viscous polymer of the alkyl aryl polyether alcohol type, is classified as a nonionic surfactant and is widely used in biomedical applications. Although tyloxapol has been reported to be cytotoxic in various cell lines, there is no published information about its possible mechanisms of cell death. Hence, the objective of this study was to determine whether tyloxapol causes apoptosis or necrosis. These data could be helpful for a better understanding of the action of tyloxapol in cellular systems.

Methods. RAW 264.7 (murine macrophage-like) cells and NIH/3T3 (mouse fibroblast) cells were treated with tyloxapol, and the activity of dehydrogenases in those cells, an indicator of cell viability, was assessed. The cell morphology changes induced by tyloxapol treatment were detected using propidium iodide nuclear staining. The hallmarks of apoptotic cells were characterized using DNA fragmentation assays, DNA fluorescence staining, and then flow analysis.

Results. Tyloxapol treatment produced dose- and time-dependent cytotoxicity. Tyloxapol treatment damaged RAW 264.7 cells more than it damaged NIH/3T3 cells. All the cells exposed to tyloxapol showed some morphological features of apoptosis, such as chromatin condensation and cell shrinkage. Typical apoptotic ladders were observed in DNA extracted from tyloxapol-treated cells. Flow cytometric analysis revealed an increase in the hypodiploid DNA population (sub-G1), indicating that DNA cleavage occurred after tyloxapol treatment. In addition, we showed that pretreating cells with zVAD-fmk, a general caspase inhibitor, did not prevent tyloxapol-induced apoptosis. The cytotoxicity of tyloxapol can be reduced by adding a nontoxic lipid 1,2-dipalmitoyl-*sn*-glycero-3-phosphocholine to attenuate the interaction of tyloxapol with the cell membrane.

Conclusions. Our results indicate that tyloxapol induces apoptosis in RAW 264.7 and NIH/3T3 cells. These data provide a novel insight into the cytotoxic action of tyloxapol at the molecular level.

KEY WORDS: apoptosis; cytotoxicity; surfactant; tyloxapol.

INTRODUCTION

Tyloxapol (Triton WR-1339) is a nonionic surfactant oligomer widely used in biomedical applications *in vitro* and *in vivo*, e.g., in contact-lens detergent, mucolytic agents for pulmonary diseases, inflammatory modulators for endotoxin-induced activations, components for drug-delivery systems and synthetic-lung surfactants, a model of hyperlipidemic atherogenesis, and a powerful up-regulator of dendrimer-mediated transfection (1–8). Recently, *in vitro* biomedical

applications for tyloxapol have been used to prevent reactions to endotoxin-induced activations in immune cells (mostly macrophages) (3,9,10). Also, tyloxapol has been used to augment nonviral gene transfer in a variety of eukaryotic cells, especially primary cells [e.g., human lung (NHBE) and porcine vascular endothelial (YPE) cells] that are difficult to transfect (5). Surfactants are known to interact with cell membranes, and tyloxapol has been reported to be toxic in epithelial and red blood cells (4,11). Also, the risk of pulmonary hemorrhage has been reported to increase after intratracheal treatment with colfosceril palmitate HSE (dipalmitoylphosphatidylcholine; Exosurf Neonatal; Glaxo-SmithKline, Middlesex, UK) in extremely low-birth-weight infants with respiratory distress syndrome. This risk may be related to the cytotoxicity of tyloxapol (11). However, the mechanism it uses to induce cell death remains unknown.

The two major causes of cell death are necrosis and apoptosis (12). Necrosis is related to an inflammatory and a degenerative process (13). Cells undergoing necrosis characteristically illustrate mitochondrial swelling, lose membrane integrity, turn off metabolism, and release a cytoplasmic component that stimulates an inflammatory response. Apo-

¹ Graduate Institute of Pharmaceutical Science, Chia Nan University of Pharmacy and Science, 60 Erh-Jen Road, Sec. 1, Jen-Te, Tainan 717, Taiwan.

² Department of Microbiology and Immunology, Medical College of Chung Shan Medical University, 110, Sec. 1, Jianguo Road, Taichung, Taiwan.

³ Department of Biotechnology, Chia Nan University of Pharmacy and Science, 60 Erh-Jen Road, Sec. 1, Jen-Te, Tainan 717, Taiwan.

⁴ To whom correspondence should be addressed. (e-mail: kuojunhua@yahoo.com.tw)

ptosis is a form of programmed cell death characterized by cytoplasmic blebbing, condensation of nuclear chromatin, DNA fragmentation, exposure of phosphatidylserine residues on the outer leaflet, and cellular fragmentation into membrane apoptotic bodies (14,15). Tyloxapol has caused cell lysis or membrane porosity in previous studies, but tyloxapol-induced apoptosis has not been previously reported (4,5,11).

The aim of this study was to determine, by examining the changes cells undergo with various dosages of tyloxapol, whether tyloxapol causes apoptosis or necrosis. These data might be helpful for a better understanding of the action of tyloxapol in cellular systems.

MATERIALS AND METHODS

Materials

Propidium iodide (PI), 1,2-dipalmitoyl-*sn*-glycero-3-phosphocholine (DPPC), and tyloxapol (T8761, Lot No. 084K1287) were obtained from Sigma-Aldrich (St. Louis, MO, USA). The stock solution of tyloxapol was freshly prepared in phosphate-buffered saline (PBS) at 10 mg/mL, which is well above its critical micelle concentration (16). The resulting solution was passed through a 0.45- μ m filter and then further diluted to desired concentrations with culture

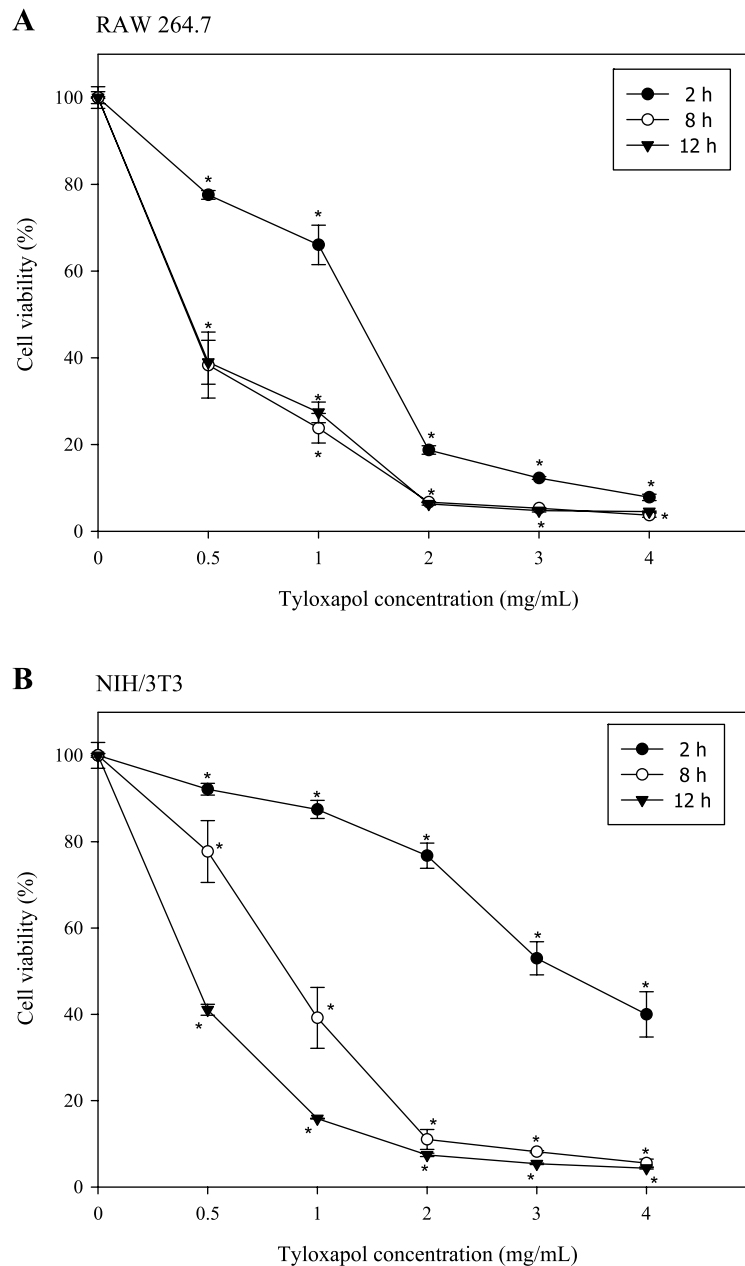


Fig. 1. Cytotoxicity assays of tyloxapol on (A) RAW 264.7 murine macrophage-like cells and (B) NIH/3T3 mouse fibroblast cells by measuring generated dehydrogenases. Negative control cells were grown without adding tyloxapol. Results are reported as cell viability percentage (average OD/average negative control OD) \pm SD ($n = 6$). * $p < 0.05$ relative to negative controls.

Table I. Inhibitory Concentrations of Tyloxapol Required for 50% Inhibition (IC_{50})

Incubation time (h)	IC_{50} (mg/mL)	
	RAW 264.7 cells ^a	NIH/3T3 cells ^b
2	1.3	3.2
8	0.4	0.9
12	0.4	0.4

^a Mouse macrophages.^b Mouse fibroblasts.

medium. The general caspase inhibitor zVAD-fmk (benzylloxycarbonyl-Val-Ala-Asp-fluoromethylketone) was obtained from Promega Corporation (Madison, WI, USA).

Cells

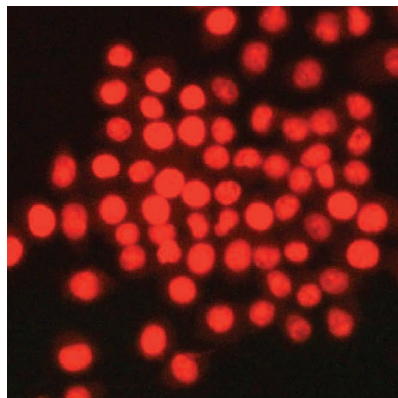
A RAW 264.7 (murine macrophage-like) cell line was maintained in RPMI 1640 medium (Gibco, Grand Island, NY, USA) supplemented with 10% heat-inactivated fetal bovine serum (FBS) and 100 U/mL penicillin/100 µg/mL streptomycin (Sigma). NIH/3T3 (mouse fibroblast) cells were grown in

Dulbecco's Modified Eagle Medium supplemented with antibiotics (penicillin and streptomycin) and 10% FBS.

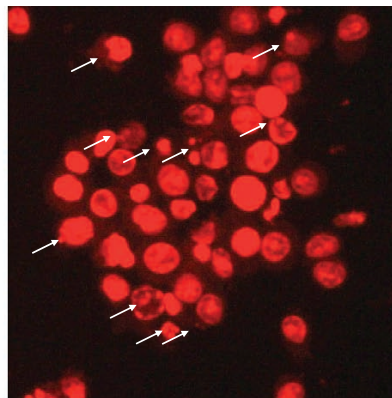
Cytotoxicity Assay

Cells were seeded in 96-well plates at 20,000 cells/100 µL/well and then incubated overnight at 37°C in an atmosphere containing 5% CO₂. Various concentrations of tyloxapol were added to the experimental cells and then incubated for various time periods. Negative control cells contained no tyloxapol. To measure cell viability, 10 µL of a cell-counting kit solution, a tetrazolium salt that produces a highly water-soluble formazan dye upon biochemical reduction in the presence of an electron carrier (1-Methoxy PMS; Cell Counting Kit-8; Dojindo Laboratories, Tokyo, Japan), was added to each well and incubated for 1–4 h. The amount of the yellow formazan dye generated by dehydrogenases in cells is directly proportional to the number of viable cells in a culture medium. The absorbance at 450 nm was obtained using an enzyme-linked immunosorbent assay reader with a reference wavelength of 595 nm. Results are reported as cell viability percentage (average OD/average negative control OD) ± standard deviation (SD).

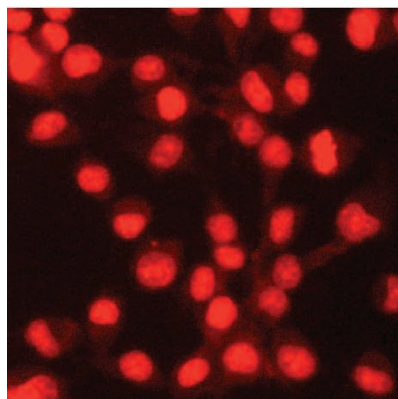
A RAW 264.7 (Control)



B RAW 264.7 (Tyloxapol 2mg/mL)



C NIH/3T3 (Control)



D NIH/3T3 (Tyloxapol 2mg/mL)

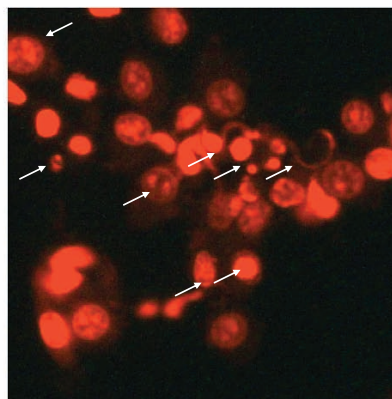


Fig. 2. Morphology changes of RAW 264.7 cells and NIH/3T3 mouse fibroblast cells induced by treatment with tyloxapol. Untreated RAW 264.7 cells (A) were compared with cells treated with 2 mg/mL tyloxapol for 2 h (B). Also, untreated NIH/3T3 cells (C) were compared with cells treated with 2 mg/mL tyloxapol for 8 h (D). The hallmarks of apoptosis, such as chromatin condensation and cell shrinkage, developed after treatment with tyloxapol are indicated by arrows. Images were taken at 200× magnification.

PI Nuclear Staining

Untreated and tyloxapol-treated cells (2×10^5) were incubated and harvested. The cells were fixed with 1% paraformaldehyde for 60 min at room temperature and then washed three times with 0.1% Tween 20 in PBS. The cells were then incubated with PI staining solution (40 $\mu\text{g}/\text{mL}$ PI, 100 $\mu\text{g}/\text{mL}$ RNase A) for 30 min in the dark. The cells were washed five times with PBS and then viewed under a fluorescent microscope (CKX 41; Olympus, Tokyo, Japan).

DNA Fragmentation Assays

Cells (1×10^6) treated with tyloxapol were washed twice with PBS, suspended in 500 μL of lysis buffer (20 mM Tris, 10 mM EDTA, 0.2% Triton X-100; pH 8.0), and incubated on ice for 10 min. After centrifugation at 1200 rpm for 10 min, the cell lysate was incubated with proteinase K (Sigma; final concentration = 200 $\mu\text{g}/\text{mL}$) to digest protein at 50°C for 8 h and then further incubated with RNase A (Sigma; final concentration = 100 $\mu\text{g}/\text{mL}$) to digest RNA at 37°C for 6 h. DNA was extracted twice, once using saturated phenol solution and then using chloroform plus isoamyl alcohol. After centrifugation at 12,000 rpm for 10 min, glycogen (Sigma; final concentration = 20 $\mu\text{g}/\text{mL}$) and an equal volume of isopropanol were added to the upper aqueous layer. The mixture was stored at -20°C for 24 h. The extracted DNA was then dissolved in TE buffer solution (10 mM Tris, 1 mM EDTA; pH 8.0) and subjected to 2% agarose gel electrophoresis at 100 V for 30 min. The experiments were repeated three times to ensure the reproducibility of the assays.

DNA Content

Untreated cells and tyloxapol-treated cells (1×10^6) were fixed with a solution containing 70% ethanol and 30% PBS at 4°C for 12 h. The cells were then centrifuged to remove the fixation solution. The cell pellets were incubated with 0.5 mL of DNA staining solution (40 $\mu\text{g}/\text{mL}$ PI, 100 $\mu\text{g}/\text{mL}$ RNase A) for 30 min in the dark. Ten thousand cells per sample were analyzed using flow cytometry (FACSCalibur; Becton Dickinson, Mountain View, CA, USA) with argon ion laser excitation at 488 nm. Data were acquired and processed using Cell Quest software (Becton Dickinson) and WinMDI software (version 2.8; The Scripps Research Institute, La Jolla, CA, USA).

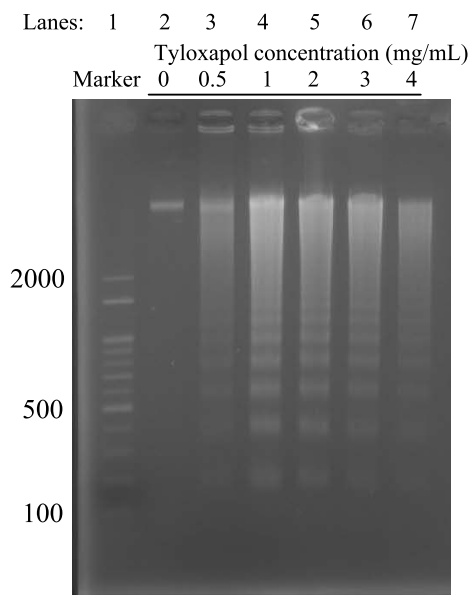
zVAD-fmk Inhibition

To study the effect of zVAD-fmk on tyloxapol-induced apoptosis, cells (1×10^6 ; untreated or pretreated with 40 μM zVAD-fmk at 37°C for 4 h) were treated with tyloxapol at 37°C. Cells were then stained with PI fixation solution as described above and analyzed using flow cytometry. The positive control of zVAD-fmk potency was confirmed by treating the cells with C_2 -ceramide (40 μM , *N*-acetyl-sphingosine; BIOMOL International L.P., Plymouth Meeting, PA, USA) under the same conditions as in the tyloxapol experiments.

Statistical Analysis

Statistical analyses were performed using a one-way analysis of variance (ANOVA) with a significance level of 0.05. The data with tyloxapol-treated cells at different dosages were compared with the data from untreated cells at each corresponding incubation time. Results are given as means \pm SD.

A RAW 264.7



B NIH/3T3

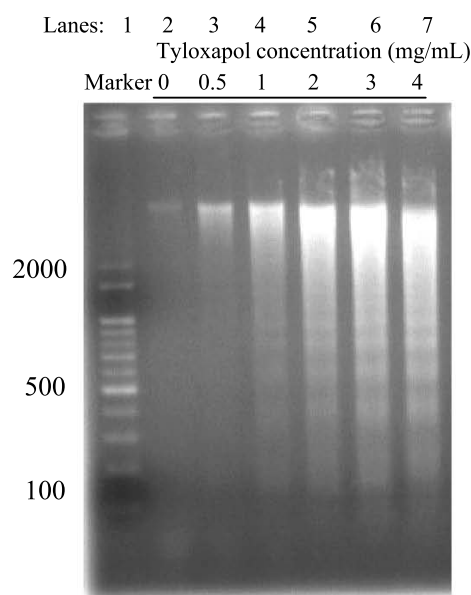


Fig. 3. Agarose gel electrophoresis of DNA extracted from (A) RAW 264.7 cells and (B) NIH/3T3 mouse fibroblast cells treated with tyloxapol for 8 h. Lane 1: DNA marker; lane 2: control (untreated cells); lanes 3–7: treated with 0.5, 1, 2, 3, and 4 mg/mL tyloxapol, respectively.

RESULTS

Cell Viability Assays

To assess the cytotoxic effect of tyloxapol, cells were incubated for 2, 8, and 12 h with various concentrations of tyloxapol (0.5, 1, 2, 3, and 4 mg/mL). Dehydrogenase activity was then analyzed. Tyloxapol exhibited dose- and time-dependent toxic effects on cell proliferation (Fig. 1). In RAW 264.7 cells, viability decreased dramatically with increased time and dosage (Fig. 1A). Subsequently, the inhibitory concentrations (IC_{50}) were interpolated from Fig. 1A for each incubation time (Table I). Results were similar in NIH/3T3 cells (Fig. 1B and Table I), except that they required longer incubation times and had higher IC_{50} values at 2- and 8-h time points than did the RAW 264.7 cells. These results indicated that tyloxapol treatment damaged the RAW 264.7 cells more than it damaged the NIH/3T3 cells.

Tyloxapol Induced Morphological Changes in Cells

To further examine whether tyloxapol induces apoptosis, after incubation, both untreated and treated cells were stained with DNA-binding dye (PI) to detect the morphological features of apoptosis. Untreated cells were more homogeneously and less intensely stained (Fig. 2A and C) than the tyloxapol-treated cells, which showed the hallmarks of apoptosis, e.g., chromatin condensation and cell shrinkage (Fig. 2B and D, arrows). These results confirmed that tyloxapol induced apoptosis in RAW 264.7 and NIH/3T3 cells.

DNA Fragmentation Assays

In cells undergoing apoptosis, a typical ladder pattern occurs because of the activation of an endogenous endonuclease that produces DNA fragments in multiples of about 180–200 base pair (bp) units (12). Typical DNA ladders were clearly visible in cells treated with tyloxapol (Fig. 3A, lanes 3–7 and Fig. 3B, lanes 5–7), but more tyloxapol (>1 mg/mL)

was required to produce DNA fragmentation in NIH/3T3 cells (Fig. 3B) than in RAW 264.7 cells. These results correlated well with the sensitivities of cell damage shown in Fig. 1.

DNA Content and zVAD-fmk Inhibition

We used a single laser (linear PI fluorescence) flow cytometer to determine DNA-strand breaks in tyloxapol-treated cells (17). Compared with untreated cells, tyloxapol-treated cells showed a dose-dependent increase in their hypodiploid DNA population (sub-G1), a hallmark of cells undergoing apoptosis, and a simultaneous decrease in their G0/G1, S, and G2/M populations (Table II), indicating that DNA cleavage occurred after the cells had been exposed to tyloxapol. Finally, tyloxapol treatment induced a higher percentage of sub-G1 population in RAW 264.7 than in NIH/3T3 cells.

To further examine the mechanisms of cell death induced by tyloxapol, 40 μ M of the peptide caspase inhibitor zVAD-fmk was added to the culture medium for 4 h before exposing the cells to tyloxapol. zVAD-fmk treatment was non-toxic to cells (data not shown). Also, the positive control of zVAD-fmk potency was confirmed by treating cells with C_2 -ceramide to rule out the possibility of peptide degradation (Table II). Flow cytometric analysis of tyloxapol-treated cells showed no difference in the percentage of the sub-G1 population of PI-stained cells with or without zVAD-fmk pretreatment (Table II). This indicates that apoptosis induced by tyloxapol cannot be inhibited by pretreatment with zVAD-fmk.

The Phospholipid Surfactant DPPC Reduced the Cytotoxicity of Tyloxapol

Because tyloxapol is rarely used alone in pharmaceutical products for human use, DPPC, another major component of Exosurf Neonatal, was introduced to mitigate the cytotoxicity of tyloxapol. Compared with cytotoxic effects of tyloxapol

Table II. Analysis of DNA Content of RAW 264.7 Mouse Macrophage Cells and NIH/3T3 Mouse Fibroblast Cells after Treatment with Tyloxapol and Effect of zVAD-fmk on Inhibiting Apoptosis

	Sub-G1 (%)		G0/G1 (%)		S (%)		G2/M (%)	
	RAW 264.7	NIH/3T3	RAW 264.7	NIH/3T3	RAW 264.7	NIH/3T3	RAW 264.7	NIH/3T3
Untreated	4.23 \pm 1.49	3.44 \pm 1.28	54.13 \pm 2.32	59.58 \pm 2.01	25.32 \pm 1.83	24.94 \pm 1.58	16.33 \pm 1.24	12.83 \pm 1.04
1 mg/mL Tyloxapol	37.23 \pm 2.57	18.59 \pm 2.01	23.92 \pm 1.92	35.81 \pm 2.11	25.12 \pm 2.05	25.81 \pm 2.14	13.74 \pm 1.05	19.80 \pm 1.23
2 mg/mL Tyloxapol	63.25 \pm 1.58	47.35 \pm 2.38	15.32 \pm 1.37	24.33 \pm 1.56	12.05 \pm 1.06	19.32 \pm 1.35	9.39 \pm 1.02	9.01 \pm 1.31
1 mg/mL Tyloxapol + ^a	36.95 \pm 1.45	19.85 \pm 2.43	24.12 \pm 2.37	30.71 \pm 2.91	21.54 \pm 1.06	26.13 \pm 1.79	17.40 \pm 1.54	23.31 \pm 1.28
2 mg/mL Tyloxapol + ^a	65.12 \pm 2.34	47.05 \pm 3.14	13.12 \pm 1.04	25.14 \pm 2.79	12.95 \pm 1.24	17.25 \pm 1.56	10.57 \pm 1.27	8.82 \pm 1.09
40 μ M C_2 -ceramide	32.93 \pm 2.05	28.45 \pm 1.92	33.12 \pm 2.05	30.17 \pm 1.24	20.58 \pm 1.91	22.35 \pm 1.54	13.38 \pm 1.44	19.08 \pm 1.77
40 μ M C_2 -ceramide + ^a	3.18 \pm 1.04	4.89 \pm 1.53	41.92 \pm 2.11	48.24 \pm 1.05	32.45 \pm 2.08	26.93 \pm 3.21	23.56 \pm 2.75	20.90 \pm 2.16

Results are given as means \pm SD ($n = 3$).

^a + 40 μ M zVAD-fmk before incubation.

shown in Fig. 1 and Table I, adding DPPC to RAW 264.7 and NIH/3T3 cells reduced the cytotoxicity of tyloxapol (Fig. 4 and Table III). The protective effect of DPPC was more profound at a 1:2 tyloxapol/DPPC ratio than at a 1:1 ratio on RAW 264.7 cells. This finding is consistent with the finding of a previous study (4) that the cytotoxicity of tyloxapol was reduced by combining it with sodium deoxycholate, another surfactant, in Caco-2 cells.

DISCUSSION

We demonstrated, and confirmed using a variety of evidence, that tyloxapol induced apoptosis in RAW 264.7 murine macrophage-like cells and NIH/3T3 mouse fibroblast cells. First, we showed the presence of nuclear condensation and cell shrinkage in tyloxapol-treated cells. Second, a DNA fragmentation assay revealed a typical apoptotic ladder.

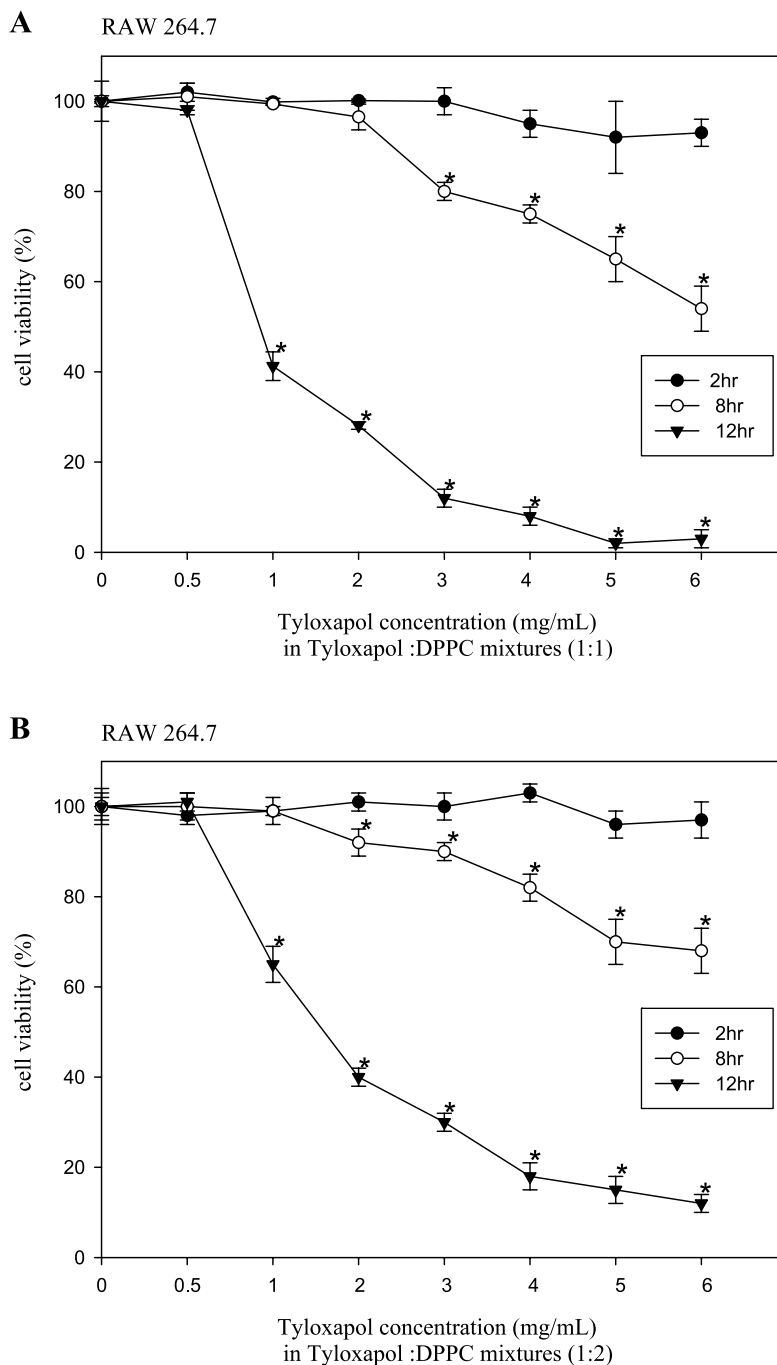


Fig. 4. Adding phospholipid [1,2-dipalmitoyl-*sn*-glycero-3-phosphocholine (DPPC)] reduced the cytotoxicity of tyloxapol on (A) RAW 264.7 murine macrophage-like cells and (B) NIH/3T3 mouse fibroblast cells. Negative control cells were grown without adding tyloxapol. Results are reported as cell viability percentage (average OD/average negative control OD) \pm SD ($n = 6$). * $p < 0.05$ relative to negative controls.

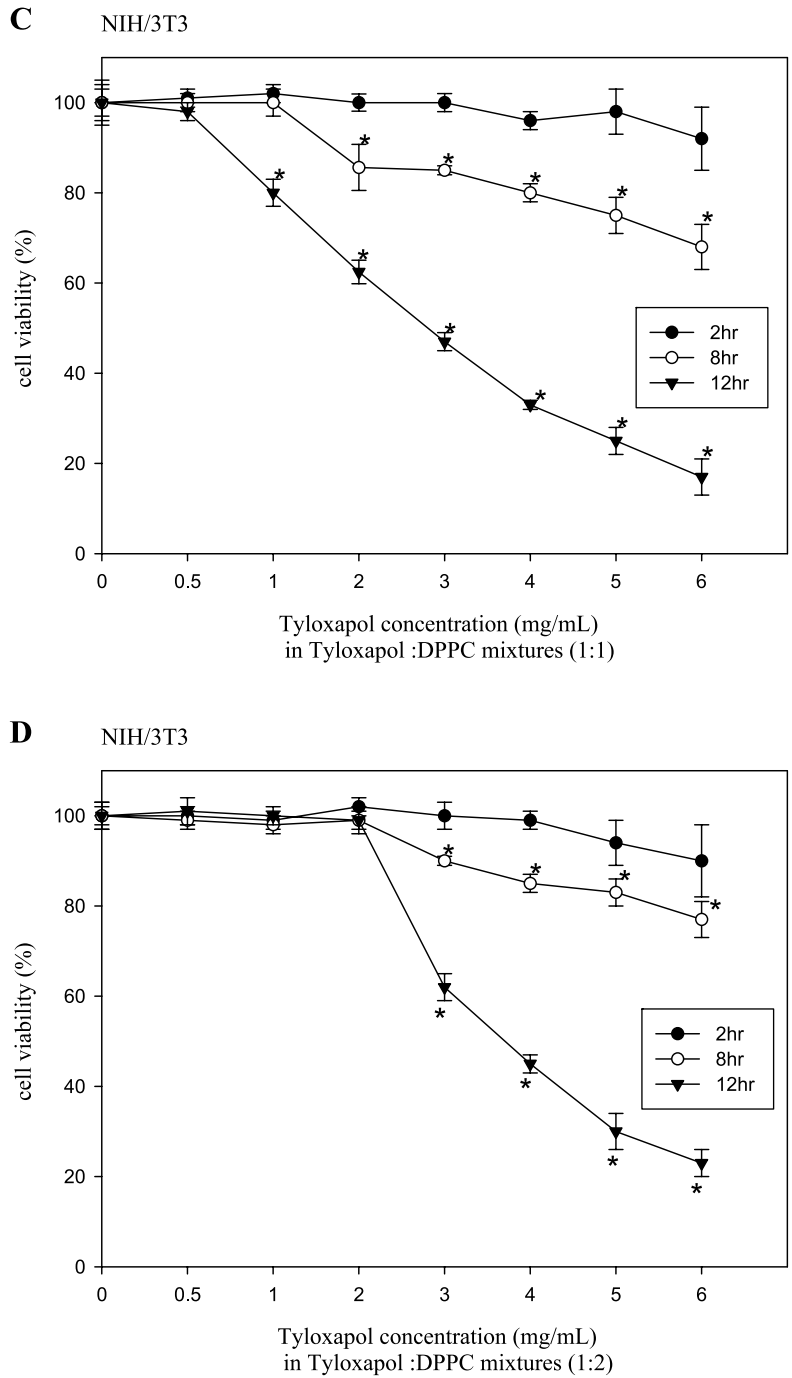


Fig. 4. Continued.

Third, an increase in the sub-G1 population in a flow cytometry analysis further confirmed the characteristics of apoptosis. Although the general caspase inhibitor zVAD-fmk irreversibly binds to the catalytic site of caspase proteases and prevents caspase-activated DNase from nicking the DNA in cultured cells (18), the present study revealed that zVAD-fmk did not block apoptosis. Our evidence is insufficient, however, to allow us to conclude that tyloxapol induces apoptosis via a caspase-independent pathway. We did observe the down-regulation of caspase 3- and -9 gene

expression (cDNA microarray analysis; unpublished data) of RAW 264.7 cells 1 h after they had been treated with 0.5 mg/mL of tyloxapol. However, we have no comparable data for NIH/3T3 cells.

The concentrations of tyloxapol used in the present study were within the range used for RAW 264.7 cells in a report by Serikov *et al.* (3), who found that tyloxapol reduced the severity of the pathologic effects of endotoxin in rabbits and protected rats from septic death after cecal ligation and puncture. However, our results revealed that tyloxapol

Table III. Inhibitory Concentrations of Tyloxapal Required for 50% Inhibition (IC_{50}) after Adding 1,2-Dipalmitoyl-*sn*-Glycero-3-Phosphocholine (DPPC)

Cell Type	IC_{50} (mg/mL)			
	RAW 264.7 ^a		NIH/3T3 ^b	
	Tyloxapal/DPPC		Tyloxapal/DPPC	
Mixture ratio				
Incubation time (h)	1:1	1:2	1:1	1:2
2	>6.0	>6.0	>6.0	>6.0
8	>6.0	>6.0	>6.0	>6.0
12	0.9	1.6	3.0	3.6

^a Mouse macrophages.

^b Mouse fibroblasts.

caused cell death by inducing apoptosis. This discrepancy may be a result of our having chosen different endpoints to detect. Cells undergoing apoptosis eventually undergo secondary necrosis after longer incubation and treatment with higher concentrations. An earlier study (5) that used tyloxapal to augment dendrimer-mediated transfection *in vitro* reported minor membrane disruption. However, increased cell lysis at high concentrations (1 and 2 mg/mL) of tyloxapal and longer incubation periods (≥ 3 h) was demonstrated in the human T cell leukemia Jurkat cell line (5). Under the same conditions, we observed that tyloxapal also induced apoptosis in Jurkat cells (data not shown). The cytotoxic effect of tyloxapal in other cell types remains to be established.

DPPC reduced the cytotoxicity of tyloxapal in RAW 264.7 and NIH/3T3 cells. DPPC proved nontoxic to cells, excluding the apoptotic effect of DPPC itself. We hypothesize that the reason for this may be the formation of mixed micelles of these two surfactants that attenuate the interaction of tyloxapal with the cell membrane. This finding is consistent with the finding of a previous study that the cytotoxicity of tyloxapal was masked in Caco-2 cells after adding the cosurfactant sodium deoxycholate to create a self-emulsifying drug delivery system (4). Tyloxapal, however, is intrinsically cytotoxic to RAW 264.7 and NIH/3T3 cells. The cytotoxic results do not contradict the *in vivo* use of tyloxapal because it is rarely used alone in clinical applications. Exosurf Neonatal, for example, contains 5–6% tyloxapal, used as an excipient.

CONCLUSIONS

In conclusion, the present study demonstrated that tyloxapal induced apoptosis in RAW 264.7 murine macrophage-like cells and NIH/3T3 mouse fibroblast cells. Also, general caspase inhibitor zVAD-fmk did not block apoptosis. The cytotoxicity of tyloxapal was attenuated by adding DPPC. These findings will contribute to a better understanding of the molecular action of tyloxapal in cellular systems.

ACKNOWLEDGMENT

This work was supported by grant NSC 94-2216-E-041-001 from the National Science Council, Taiwan.

REFERENCES

1. J. E. F. Reynolds (ed.). *Martindale, The Extra Pharmacopoeia*, 31st ed., Royal Pharmaceutical Soc., London, 1996, p. 1347.
2. A. R. Gennaro (ed.). *Remington: The Science and Practice of Pharmacy*, 19th ed., Mack, Easton, PA, 1995.
3. V. B. Serikov, T. V. Glazanova, E. H. Jerome, N. W. Fleming, H. Higashimori, and N. C. Staub Sr. Tyloxapal attenuates the pathologic effects of endotoxin in rabbits and mortality following cecal ligation and puncture in rats by blockade of endotoxin receptor–ligand interactions. *Inflammation* **27**:175–190 (2003).
4. N. Gursoy, J. S. Garrigue, A. Razafindratsita, G. Lambert, and S. Benita. Excipient effects on *in vitro* cytotoxicity of a novel paclitaxel self-emulsifying drug delivery system. *J. Pharm. Sci.* **92**:2411–2418 (2003).
5. J. F. Kukowska-Latallo, C. Chen, J. Eichman, A. U. Bielinska, and J. R. Baker. Enhancement of dendrimer-mediated transfection using synthetic lung surfactant exosurf neonatal *in vitro*. *Biochem. Biophys. Res. Commun.* **14**:253–261 (1999).
6. K. Yamamoto, B. Shen, C. Zarins, and A. M. Scanu. *In vitro* and *in vivo* interactions of Triton 1339 with plasma lipoproteins of normolipidemic rhesus monkeys. Preferential effects on high density lipoproteins. *Arteriosclerosis* **4**:418–434 (1984).
7. K. L. Dechant and D. Faulds. Colfosceril palmitate. A review of the therapeutic efficacy and clinical tolerability of a synthetic surfactant preparation (Exosurf Neonatal) in neonatal respiratory distress syndrome. *Drugs* **42**:877–894 (1991).
8. N. C. Staub, K. E. Longworth, V. Serikov, E. H. Jerome, and T. Elsasser. Detergent inhibits 70–90% of responses to intravenous endotoxin in awake sheep. *J. Appl. Physiol.* **90**:1788–1797 (2001).
9. M. J. Thomassen, J. M. Antal, L. T. Divis, and H. P. Wiedemann. Regulation of human alveolar macrophage inflammatory cytokines by tyloxapal: a component of the synthetic surfactant Exosurf. *Clin. Immunol. Immunopathol.* **77**:201–205 (1995).
10. A. J. Ghio, B. C. Marshall, J. L. Diaz, T. Hasegawa, W. Samuelson, D. Povia, T. P. Kennedy, and C. A. Piantodosi. Tyloxapal inhibits NF-kappa B and cytokine release, scavenges HOCl, and reduces viscosity of cystic fibrosis sputum. *Am. J. Respir. Crit. Care Med.* **154**:783–788 (1996).
11. R. D. Findlay, H. W. Taesch, R. David-Cu, and F. J. Walther. Lysis of red blood cells and alveolar epithelial toxicity by therapeutic pulmonary surfactants. *Pediatr. Res.* **37**:26–30 (1995).
12. G. Majno and I. Joris. Apoptosis, oncosis, and necrosis. An overview of cell death. *Am. J. Pathol.* **146**:3–15 (1995).
13. M. C. Cummings, C. M. Winterford, and N. I. Walker. Apoptosis. *Am. J. Surg. Pathol.* **21**:88–101 (1997).
14. S. W. Hetts. To die or not to die: an overview of apoptosis and its role in disease. *JAMA* **279**:300–307 (1998).
15. M. E. Bianchi and A. Manfredi. Chromatin and cell death. *Biochim. Biophys. Acta* **1677**:181–186 (2004).
16. H. Schott. Comparing the surface chemical properties and the effect of salts on the cloud point of a conventional nonionic surfactant, octoxynol 9 (Triton X-100), and of its oligomer, tyloxapal (Triton WR-1339). *J. Colloid Interface Sci.* **205**:496–502 (1998).
17. Z. Darzynkiewicz, S. Bruno, G. Del Bino, W. Gorczyca, M. A. Hotz, P. Lassota, and F. Traganos. Features of apoptotic cells measured by flow cytometry. *Cytometry* **13**:795–808 (1992).
18. M. D. Jacobsen, M. Weil, and M. C. Raff. Role of Ced-3/ICE-family proteases in staurosporine-induced programmed cell death. *J. Cell Biol.* **133**:1041–1051 (1996).